Journal of Fluids and Structures (2002) **16**(4), 529–542
doi:10.1006/jfls.2001.0435 available online at http://www.idealibrary.com on IDEAL®

AN EXPERIMENTAL STUDY OF PAPER FLUTTER

Y. WATANABE
Ryoken Tech Co., Ltd., Nagasaki, Japan

S. SUZUKI AND M. SUGIHARA
Hiroshima Research & Development Center, Mitsubishi Heavy Ind., Ltd.
Mihara, Japan

AND

Y. SUEOKA
Yokohama Research & Development Center, Mitsubishi Heavy Ind., Ltd.
Yokohama, Japan

(Received 30 June 2001, and in final form 11 September 2001)

An experimental study was conducted in order to clarify the phenomenon of paper flutter. Flutter speed was measured in wind tunnel tests for sheet paper and web paper of various materials, sizes and tensions. The relationships between flutter speed, rigidity, mass ratio and tension were clarified from a large data set. The flutter boundaries were obtained in the form of dimensionless flutter speed and mass ratio for the case of sheet paper, and dimensionless flutter speed, mass ratio and tension parameter for the case of web paper. The flutter mode and air-flow around fluttering paper were investigated by visualization tests.

1. INTRODUCTION

PAPER HAS MANY USES besides that as a medium of information, and the demand for paper is increasing with global cultural and economic development. Global demand will continue to grow in the future, even though there is a trend toward a paperless society due in part to the increased use of computers. Figure 1 shows the circulation of newspapers in Japan as an example of the growth in demand for paper. The circulation trends of magazines, books and leaflets seem to be similar to that of newspapers. The production capacity of printing presses and paper machines continues to increase, indicating that the speed of these machines is also increasing. Figure 2 shows the advances in maximum paper machine speed; see, e.g., Antos (1989) and Nagano (1999). The maximum speed of a newsprint machine has reached about 1800 m/min (30 m/s) at present. With increasing operation speed, the speed of the air-flow around paper during processing increases, and flutter occurs.

Flutter causes wrinkles and folds in the paper, resulting in a lowering of production quality. In a severe case of flutter, the paper may be broken, causing the machine to shut down. Flutter is one of the most significant obstacles that need to be overcome in order to improve the performance of printing presses and paper machines. However, the phenomenon is not well understood, which makes it very difficult to predict the occurrence of flutter and to take appropriate countermeasures. In this context, the authors

0889-9746/02/040529 + 17 $35.00/0

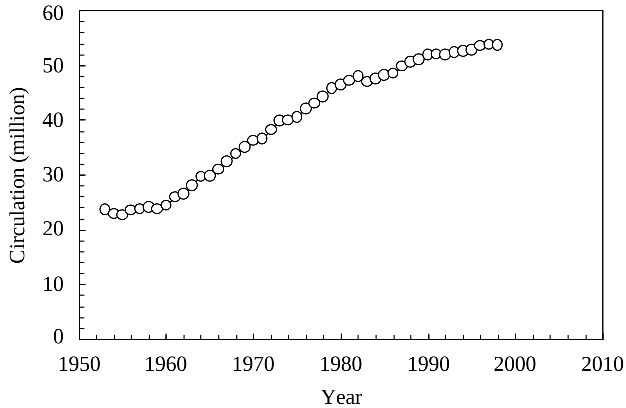

Figure 1. Circulation of newspaper in Japan.

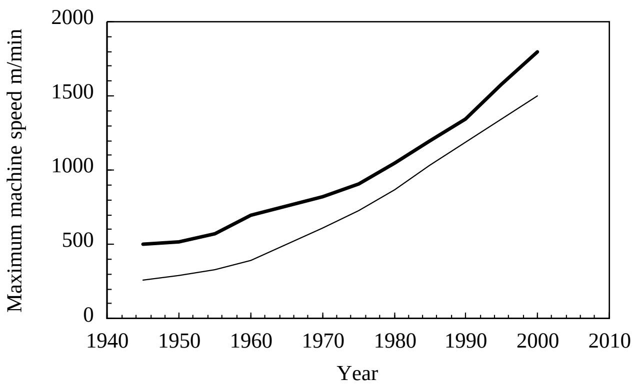

Figure 2. Progress in maximum paper machine speed:—, newsprint; —, publication paper.

have been conducting experimental and analytical studies since around 1990 in an attempt to clarify the mechanism of flutter and the primary factors that influence the flutter speed; see, e.g., Watanabe *et al.* (1991, 1997). This paper is a report of the experimental study.

2. PAPER FLUTTER IN PRINTING PRESSES AND PAPER MACHINES

Paper is conveyed in the form of cut paper (sheet) and continuous paper (web) in printing presses and paper machines, and paper flutter can be classified into sheet flutter and web flutter. Some examples of paper flutter in real machinery are detailed in the following.

Figure 3 shows a schematic of a sheet offset printing press. A sheet of paper is conveyed from the feeder to the printing unit, and then printed between the blanket cylinder (B) and the impression cylinder (I) sequentially with black, blue, magenta and yellow. The printed sheet is then gripped by chains and conveyed along the guide plate. Sheet flutter occurs at the corner of the guide plate. The edge of the sheet flutters violently, causing wrinkles and breakage to occur.

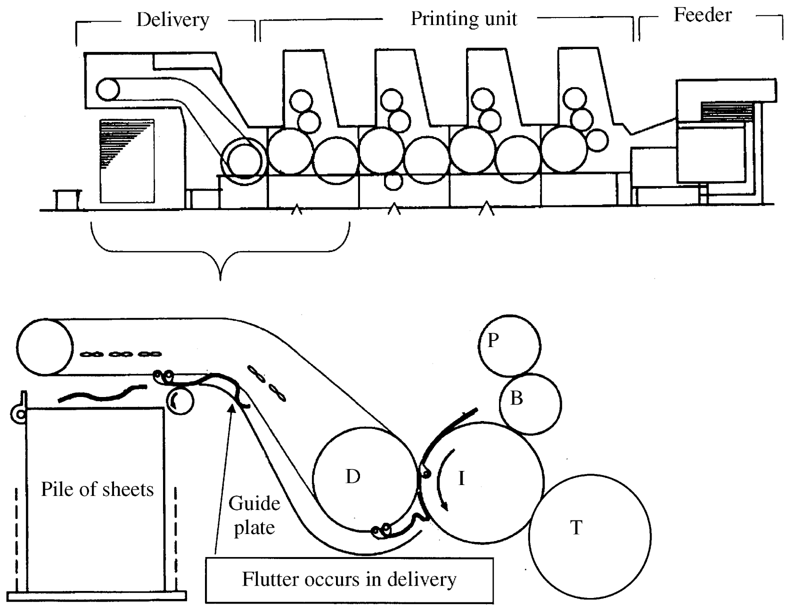

Figure 3. Sheet flutter in sheet offset press: P, plate cylinder; B, blanket cylinder; I, impression cylinder; T, transfer cylinder; D, delivery cylinder.

Figure 4 shows a photograph of sheet flutter in the folder of an offset printing press. After the web is cut into sheets, flutter occurs at the roll in the guide plate between the two cylinders; see, e.g., Watanabe *et al.* (1994). The trailing edge of the sheet is rolled up and a fold is created.

Figure 5 shows the layout of a paper machine and a side view of the dryer section in which flutter occurs. Web flutter occurs between the top and bottom cylinders, in an area called the "free-run", where no support is provided; see, e.g., Ashworth (1986) and Hill (1988). In the free-run area, a cross-flow is induced by the air movement (A) associated with dryer fabric and the airflow (B) from pocket ventilating roll. Edge flutter occurs at the outer edge of the web due to this cross-flow, as shown in Figure 6. The strength of the web in the dryer is low enough to allow the paper to be broken by edge flutter. A breakage results in significant downtime, which causes considerable financial loss to the paper processor.

3. SHEET FLUTTER TESTS

3.1. Test Method

Sheets of paper in printing presses undergo many complicated motions, including flat motion, circular motion, and switch back. The attention of the present study is focussed on the flutter that occurs during flat motion, namely "flag-flutter". Flag-flutter is known to occur in printing presses (Figure 4) and was observed in a flutter test of sheet paper on a flat plate (Watanabe *et al.* 1994). The present data is therefore expected to be applicable for the rough estimation of flutter on the roller and guide plate. The tests were conducted in a blower-type wind tunnel, which provided a maximum test wind speed of 25 m/s in a

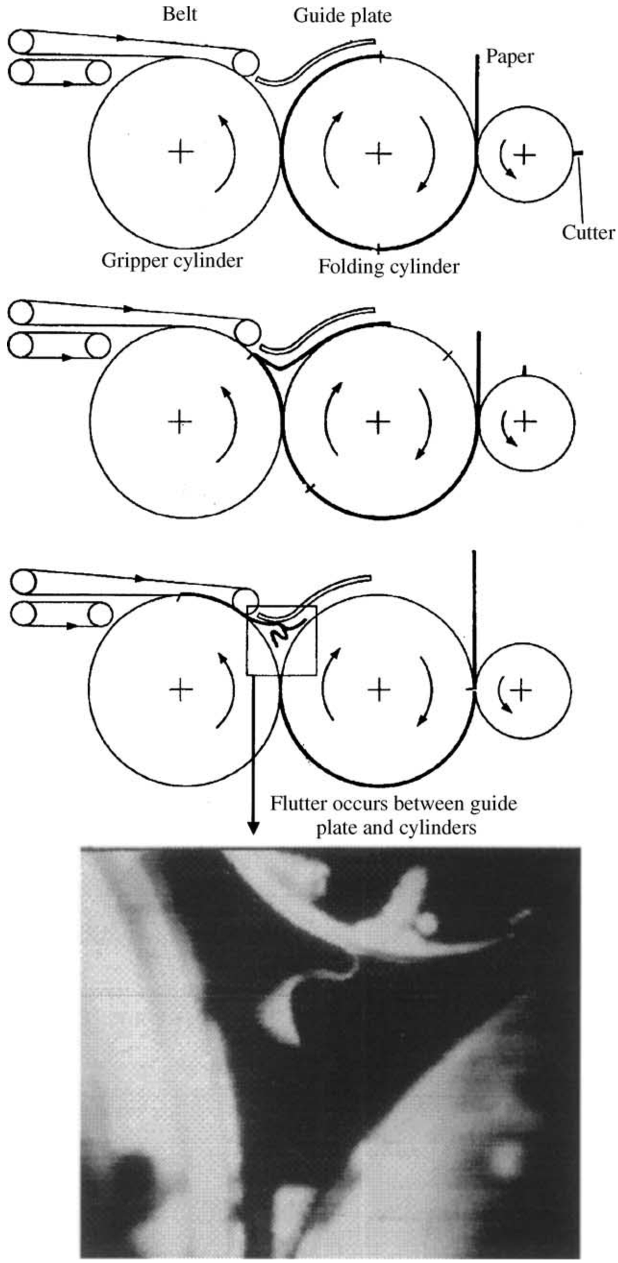

Figure 4. Sheet flutter in folder of printing press.

1 m square test-section. A sheet was installed vertically on a wire in the wind tunnel, as shown in Figure 7. Two types of paper sheets were used, flag type ($d/c = 0 \cdot 7$) and long type ($d/c = 2 \cdot 3$–$4 \cdot 0$). Tests were conducted on about 50 sheets, made of 11 kinds of paper and 3 kinds of elastic materials (aluminium, cellophane, and polyester). Figure 8 shows the relationship between the rigidity and area density of the sheet and web materials. It is interesting that the rigidity of paper is higher than that of metal and plastic for the same area density.

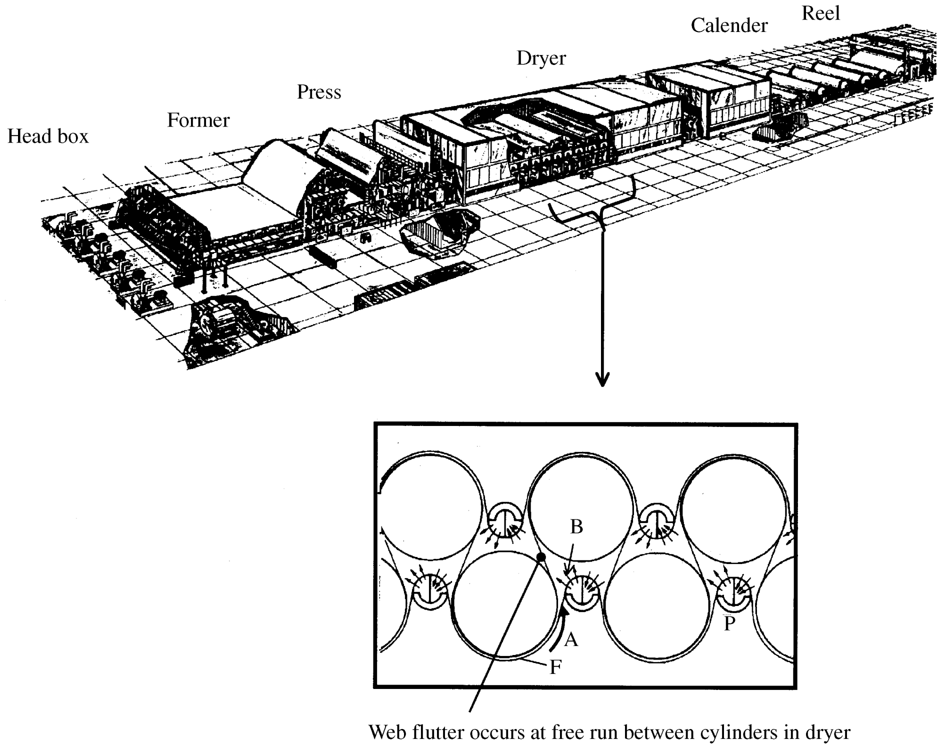

Figure 5. Web flutter in paper machine: A, air-flow from pocket ventilating roll (P); B, air-flow associated with dryer fabric (F).

3.2. Test Results

Figure 9 shows the amplitude and frequency of flutter in relation to wind speed. Flutter occurred suddenly at a certain wind speed (U_S) as the wind speed was gradually increased. Thereafter, the amplitude and frequency of flutter increased with wind speed, to the point where the sheet finally broke. Flutter did not cease at U_S when the wind speed was lowered again past the onset speed. Rather, flutter ceased at a lower wind speed, U_Q. This hysteretic behaviour can be seen in the amplitude-wind speed graph in Figure 9. The following relationship between these wind speeds was obtained from about 30 test data:

$$U_Q = 0\cdot 75\ U_s \pm 0\cdot 2$$

Figures 10(a) and (b) show U_S versus chord length (c) and U_S versus bending stiffness per unit width (*EI*), respectively. From these figures, U_S can be seen to be proportional to the -5 to -1.5 power of *c*, and also to the $0\cdot 5$ power of *EI*. Hence the dimensionless flutter speed U_S^* may be expressed as

$$U_S^* = U_S/(EI/\rho c^3)^{1/2}. \qquad (1)$$

Figure 11 shows the relationship between U_S^* and the mass ratio μ. This data was obtained from a review of previous data, Watanabe *et al.* (1991). The data of Huang (1995) and Yamaguchi *et al.* (1999) converted by equation (1) are also plotted. From the

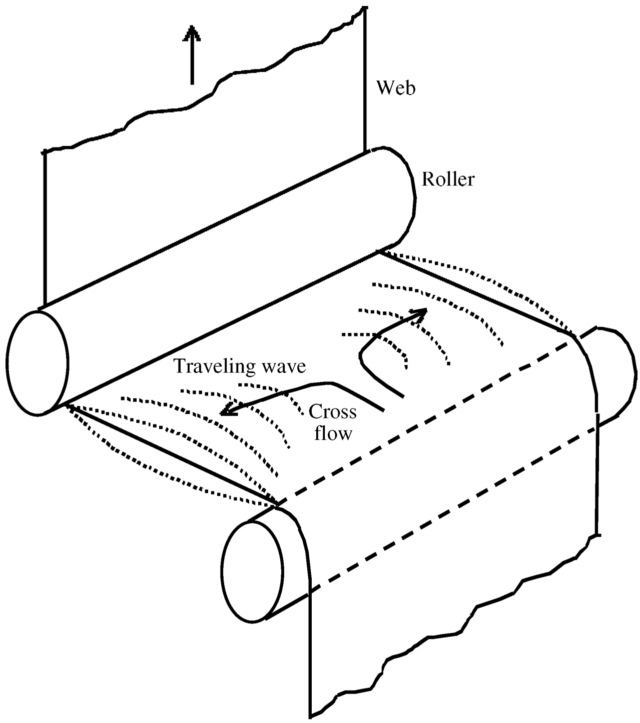

Figure 6. Edge flutter in web.

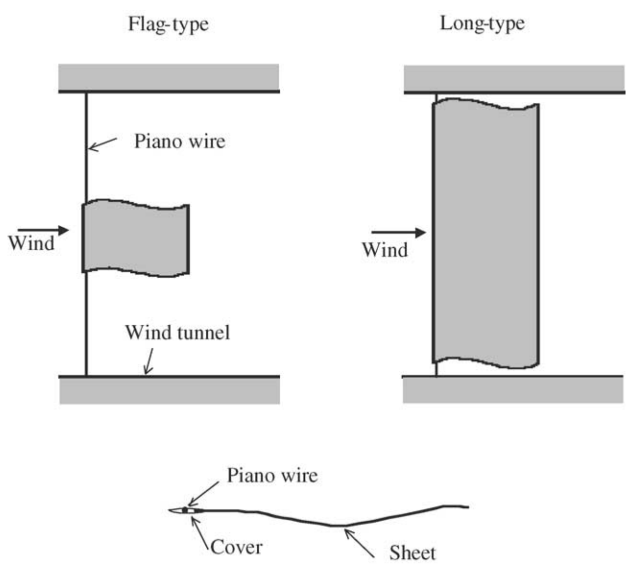

Figure 7. Sheet flutter test method.

figure, it can be seen that U_S^* tends to decrease in proportion to the $-0 \cdot 5$ to -1 power of μ. The behaviour of dimensionless flutter speed over a wide range of mass ratios was clarified by presenting data from three different studies in terms of this dimensionless formula.

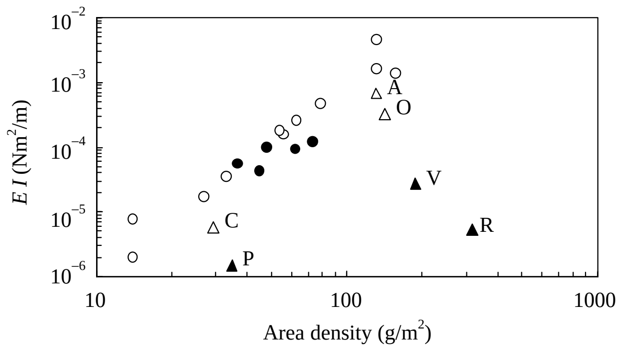

Figure 8. Relationship between rigidity and area density of sheet and web materials. Sheet: ○, paper; △A, aluminum; △O, OHP sheet; △C, cellophane. Web: ●, paper; ▲V, vinyl; ▲R, rubber; ▲P, polyethylene.

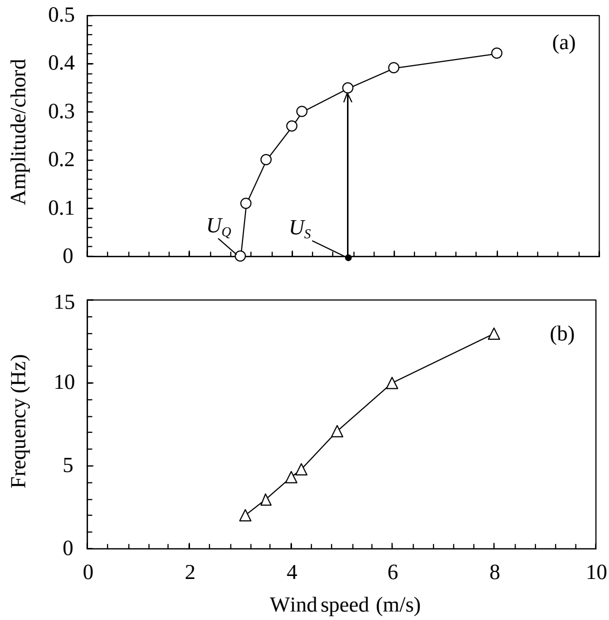

Figure 9. Amplitude and frequency of sheet flutter: (a) amplitude versus wind speed; (b) frequency versus wind speed.

The difference between flag sheet and long sheet is small. This seems to be because three-dimensional effects also appeared in the long sheet by the span-wise deformation.

3.3. Visualization of Flutter Mode

The flutter mode was recorded by a camera using a multi-strobe light and a black sheet of paper with a white line drawn down the centre. Two kinds of papers were used in the test; thin paper (0.028 mm thickness) and thick paper (0.235 mm thickness). Figure 12 shows photographs of the observed flutter. In the case of the thin sheet, the white line is intermittent because the sheet exhibited complex three-dimensional motion. By contrast, the thick sheet exhibited regular two-dimensional motion. Travelling waves were observed in both sheets.

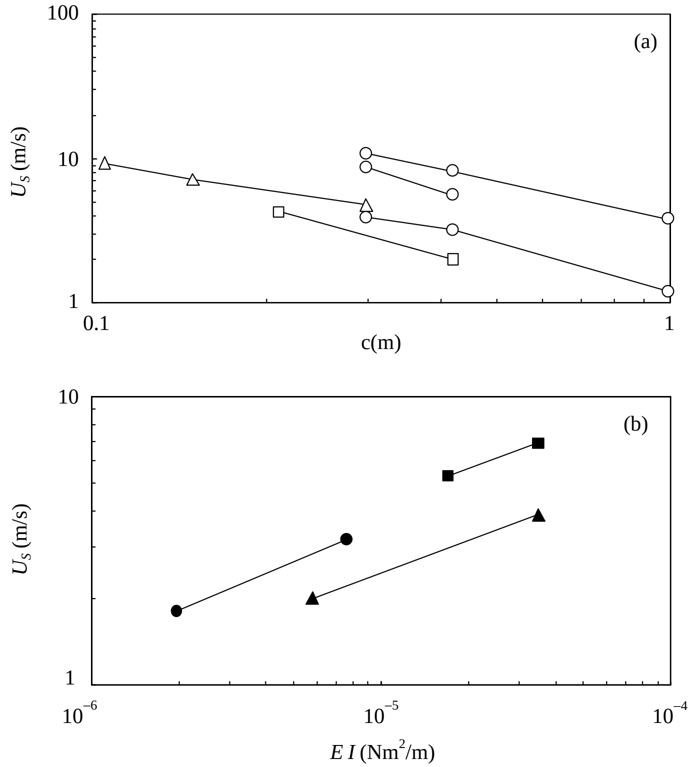

Figure 10. Sheet flutter speed versus chord length and rigidity. (a) U_W versus c: ○, paper; □, polyester; □, cellophane. (b) U_W versus EI: ●, $\mu = 0.028$; ▲, $\mu = 0.0580{-}0.0650$; ■, $\mu = 0.076{-}0.093$.

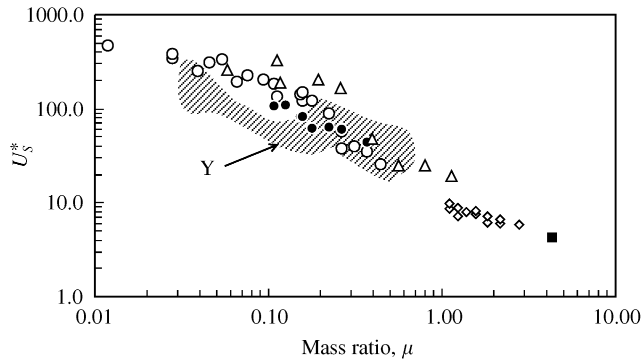

Figure 11. Dimensionless flutter speed of sheet. Present data: ○, flag-type paper; ●, long-type paper; △, elastic sheet. Other data: ■, Kornecki *et al.* (1976); ♦, Huang (1995); **Y**, Yamaguchi *et al.* (1999).

3.4. Visualization of Air-flow around a Sheet

The air-flow around the fluttering sheet was observed using the smoke wire method. A stainless-steel wire of 0.2 mm diameter was stretched at right angles to the sheet surface and then coated with paraffin oil mixed with aluminium powder. Smoke streamlines were

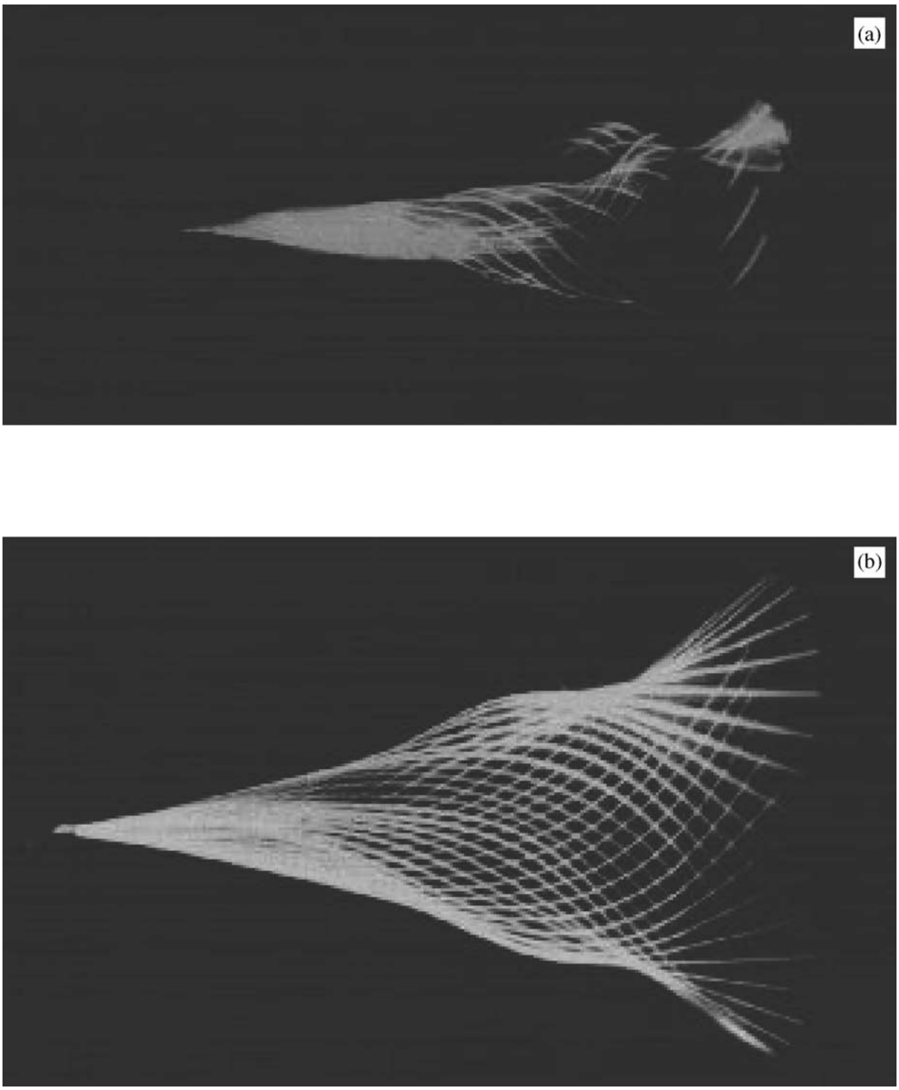

Figure. 12. Sheet flutter modes by visualization test: (a) thin paper ($\mu = 0.028$); (b) thick paper ($\mu = 0.37$).

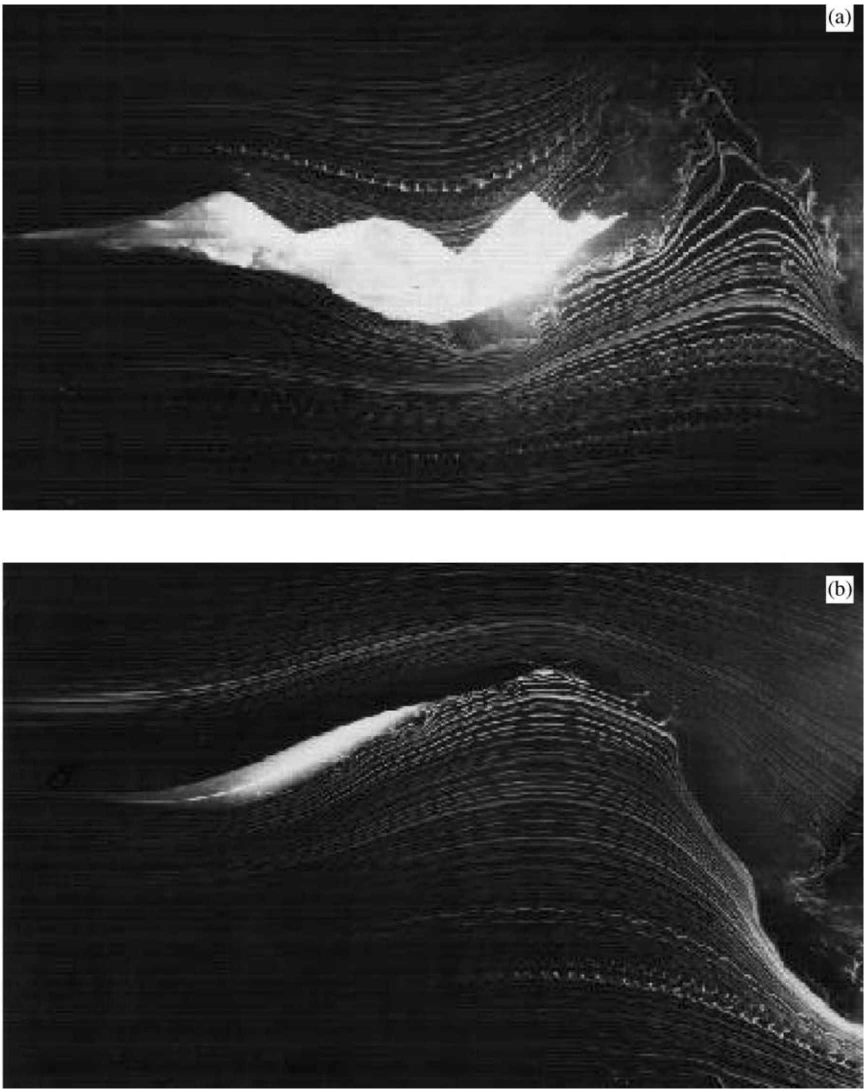

Figure 13. Air-flow around sheet by smoke-wire method: (a) thin paper ($\mu = 0.028$); (b) thick paper ($\mu = 0.37$).

generated by applying an electric current to the wire. The same thin and thick sheets as used in the mode visualization test were used in this test.

The photographs of air-flow are shown in Figure 13. There are small-scale vortices around the fluttering sheet; however, the air-flow along the curved surface of the sheet does not exhibit large-scale separation. Notably, the air-flow around the thick sheet is similar to a potential flow. The complex three-dimensional motion of the thin sheet can also be observed in this flow photograph. Vortices appear to be more abundant around the thin sheet, probably because of the three-dimensional motion of this sheet.

4. WEB FLUTTER TESTS

4.1. Test Method

A flutter test was conducted using the moving web simulator, in which cross-flow from an air nozzle impinged on a moving web, as shown in Figure 14(a). The results confirmed

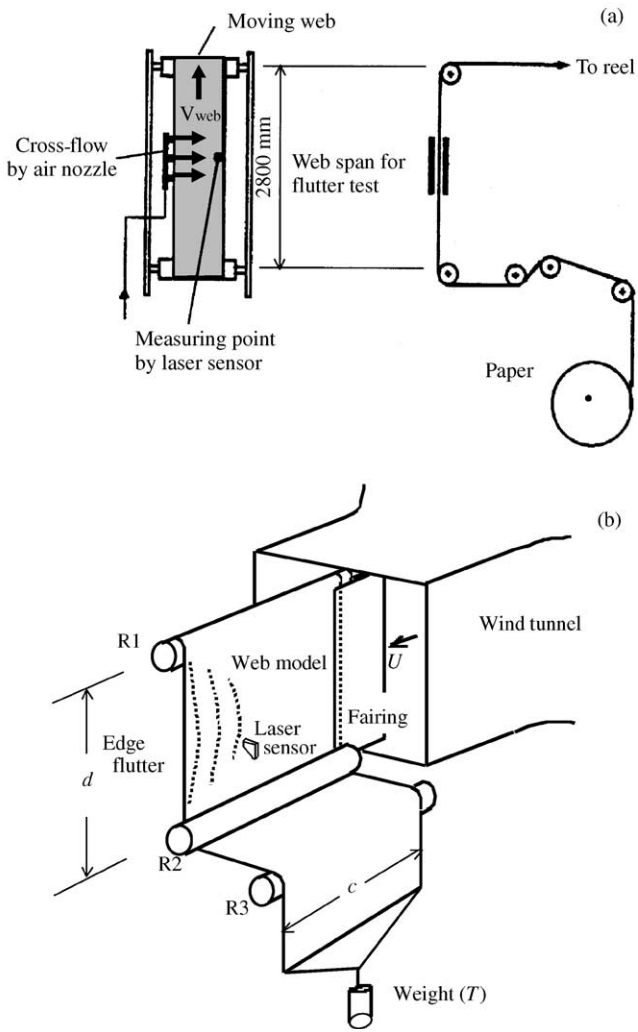

Figure 14. Web flutter test method: (a) flutter test by moving web simulator; (b) flutter test by static web

that flutter speed is not influenced by the speed of the moving web. Hence, web flutter can be simulated by a static web test. Tests for a parametric study were performed using the static web in the wind tunnel, as shown in Figure 14(b). The static web model was supported vertically by three rolls (R1, R2, R3). The upper end of the web was fixed to R1 with tape, and a tensile weight was attached at the lower end. The fairing was made of aluminium plate and installed at the leading edge of the web such that flutter occurs at the trailing edge. The amplitude of flutter at the centre of the trailing edge was measured by a laser sensor. Tests were conducted on 63 webs with varying web span (d), web width (c), and tension (T) for five kinds of papers and three kinds of elastic web materials (see the relationship between rigidity and area density in Figure 8).

4.2. Test Results

An example of the amplitude and frequency data obtained is shown in Figure 15 against wind speed. The amplitude of flutter increases gradually and monotonically with increasing wind speed. It is notable that the hysteresis with respect to flutter onset/cessation that was observed in sheet flutter was not observed in web flutter. It is difficult to determine the exact web flutter speed, because amplitude increases gently from zero. Hence, the web flutter speed is defined as the wind speed at which the r.m.s. amplitude of flutter reaches 1 mm. Flutter frequency increases with increasing wind speed in the same way as seen for sheet flutter.

The influence of each of the number of parameters on flutter speed, and the characteristics of the dimensionless flutter speed are examined as follows. Figure 16 shows web flutter speed (U_W) versus span (d), rigidity (EI), and tension (T). The following

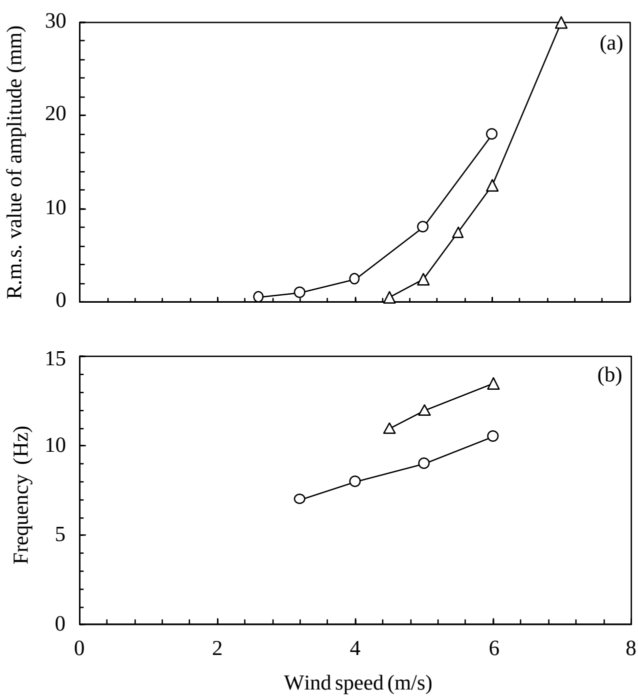

Figure 15. (a) Amplitude versus wind speed; (b) frequency versus wind speed: ○, $T = 12.4$ N/m; △, $T = 70$ N/

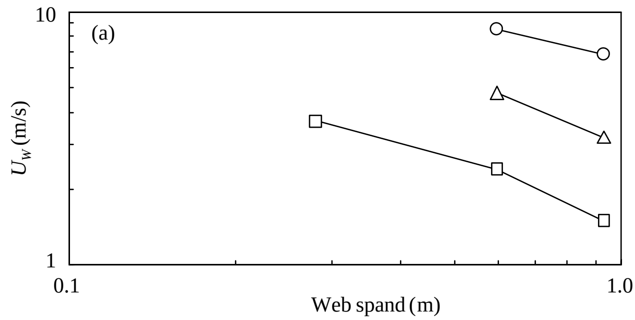

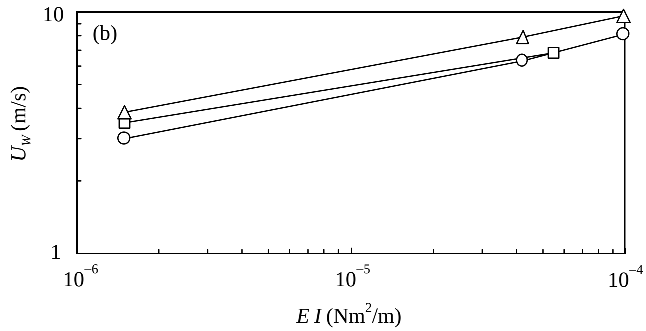

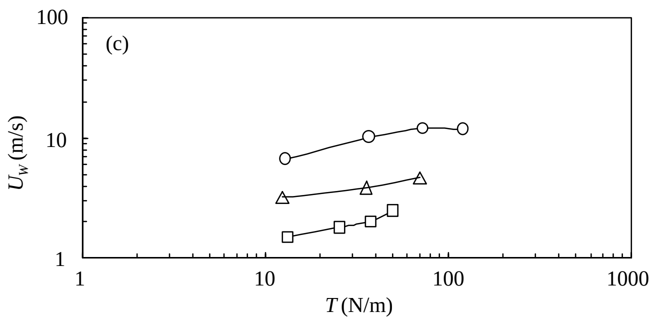

Figure 16. Web flutter speed versus span (d), rigidity (EI) and tension (T): (a) U_W versus d ($T = 11$–12 N/m); $\bigcirc$, paper; $\triangle$, vinyl; $\square$, rubber: (b) U_W versus EI; $\bigcirc$, $T = 14$–15 N/m; $\triangle$, $T = 29$–34 N/m; $\square$, $T = 40$–43 N/m: (c) U_W versus T; $\bigcirc$, paper; $\triangle$, vinyl; $\square$, rubber.

relations were obtained from this figure:

$$U_W \propto d^{\alpha}, \quad U_W \propto (EI)^{\beta}, \quad U_W \propto T^{\gamma},$$

where $\alpha = -1 \cdot 0$ to $-1 \cdot 3$, $\beta = 1/6$ to $1/3$ and $\gamma = 1/4$ to $1/2$.

The length c was observed to have no effect on web flutter speed in any of the test conditions. The dimensionless web flutter speed can be then defined as follows:

$$U_W^* = U_W/(EI/\rho d^3)^{1/2}. \tag{2}$$

Tension is a necessary consideration in the analysis of web flutter, in addition to the mass ratio. The following parameter is then introduced to incorporate tension:

$$\Gamma = \mu(Td^2/EI)^{-1}. \tag{3}$$

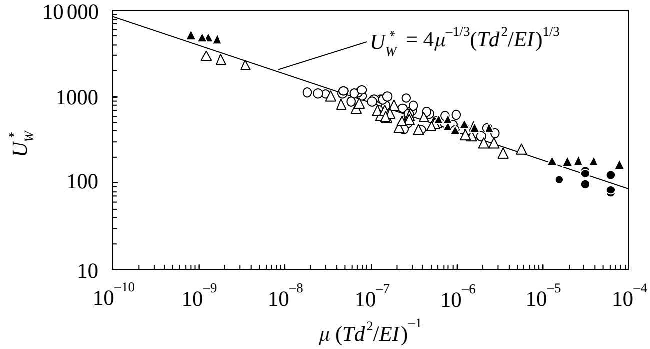

Figure 17. Dimensionless flutter speed of web. Present data: ○, paper: △, plastic: Chang (1990) data: ●, paper; ▲, plastic.

The relationship between U_W^* and Γ is shown in Figure 17. Data from Chang (1990) converted according to equations (2) and (3) are also plotted in Figure 17. The data sets correlate very well, with minimal dispersion. The empirical equation proposed for this relationship is written as

$$U_W^* = 4\Gamma^{-1/3} = 4\mu^{-1/3}(Td^2/EI)^{1/3}. \tag{4}$$

From equations (2) and (4), U_W then becomes

$$U_W = 4(m/\rho d)^{-1/3}(Td^2/EI)^{1/3}(EI/\rho d^3). \tag{5}$$

Equation (4) is represented by a solid line in Figure 17.

4.3. Visualization of Flutter Mode and Air-Flow around Web Paper

Figure 18 shows photographs of the flutter mode and air-flow around web paper. Travelling waves can be observed in this mode of flutter. Vortices due to separation of the

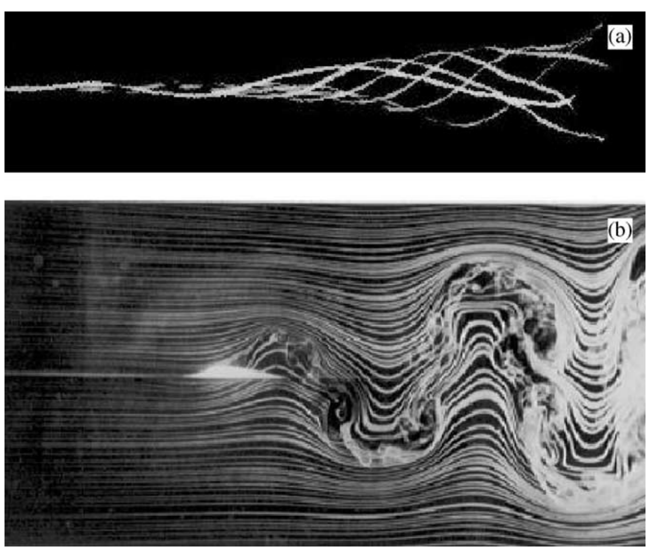

Figure 18. (a) Web flutter mode; (b) air-flow around web.

air-flow are not observed around the web; however, large circulation vortices caused by the motion of the trailing edge can be seen to grow in the wake.

It is remarked that the flutter modes in Figures 12(b) and 18(a) are remarkably similar to those of a cantilevered pipe conveying fluid (Païdoussis 1998).

5. CONCLUSION

An experimental study was conducted in order to clarify the behaviour of paper flutter and the primary factors that affect flutter speed using wind tunnel tests. The results are summarized as follows.

Sheet flutter amplitude is shown to exhibit some degree of hysteresis with respect to increasing and decreasing wind speed. Web flutter does not exhibit this hysteretic behaviour; instead, the web flutter amplitude increases gradually and monotonically with increasing wind speed.

Flutter frequency was found to increase with wind speed in both sheet and web forms, and the flutter motion was observed to consist of travelling waves. No significant air-flow separation was observed around fluttering paper, and air-flow was similar to potential flow. These characteristics of frequency, flutter mode and air-flow hold qualitatively for both sheet and web paper.

The primary factors that influence sheet flutter were found to be $EI/\rho c^3$ and the mass ratio ($m/\rho c$), and web flutter was found to be additionally influenced by a tension parameter (Td^2/EI). The flutter boundaries with respect to wind speed were obtained in the form of dimensionless flutter speed and mass ratio (in the case of sheet paper, Figure 11) and dimensionless flutter speed, mass ratio and tension parameter (in the case of web paper, Figure 17).

ACKNOWLEDGEMENT

The authors are very grateful to Dr K. Isogai for helpful suggestions and for reviewing the manuscript, and to Mr H. Kunimaru for assisting in the experiments.

REFERENCES

ANTOS, D. 1989 Papermaking in the 21st century. *Paper Age*, December, 22 pages.

ASHWORTH, T.N. 1986 Improving sheet control in the dryers Part—sheet disturbance—an analysis of the forces. *TAPPI Papermakers Conference*, New Orleans, pp. 247–260.

CHANG, Y.B. 1990 An experimental and analytical study of web flutter. Ph. D. thesis, Oklahoma State University, OK, U.S.A.

HILL, K.C. 1988 Dryer sheet stability for older paper machines. *TAPPI Journal*, **71**(8), 55–59.

HUANG, L. 1995 Flutter of cantilevered in axial flow. *Journal of Fluids and Structures* **9**, 127–147.

NAGANO, A. 1999 The development and future of the paper machine technology. *The 34th Paper and Pulp Symposium*, The Society of Fiber Science and Technology, Tokyo.

PAÏDOUSSIS, M.P. 1998 *Fluid–Structure Interactions: Slender Structures and Axial Flow*. London: Academic Press.

WATANABE, Y. SUZUKI, S. SUEOKA & Y. KUNIMARU, H. 1991 The flutter mechanism of sheet. *Proceeding of the First International Conference on Web Handling*, Oklahoma State University, Stillwater, OK, U.S.A., pp. 246–256.

WATANABE, Y., KONO, K., SUEOKA & Y., MAKIOKU, N. 1994 Stabilization of paper behaviour in folder of printing press. Mitsubishi Juko Giho **31**, 87–90.

WATANABE, Y., ISOGAI, K., SUZUKI, S. & SUGIHARA, M. 1997 Analysis of paper sheet flutter. *Second International Conference on Flow Interaction cum Exhibition /Lectures on Interaction of Science & Art*, Berlin, pp. 45–47.

YAMAGUCHI, N., YOKOTA, K. & TSUJIMOTO, R. 1999 Fluttering behaviour of a flexible thin sheet in high-speed flow. (2) Test results and predicted behaviors for low mass ratios. *Nihon Kikai Gakkai Ronbunshu*, **65**, 1232–1239.

APPENDIX: NOMENCLATURE

c	Chord length
d	Web span
EI	Bending stiffness per unit width
m	Mass per unit area
T	Tension
U	Wind speed
U_S	Sheet flutter speed (self-excited starting point)
U_Q	Sheet flutter speed (quenching point)
U_W	Web flutter speed
U_S^*	Dimensionless sheet flutter speed (self-excited starting point), $U_S/(EI/\rho c^3)^{1/2}$
U_W^*	Dimensionless web flutter speed, $U_W/(EI/\rho d^3)^{1/2}$
V_{web}	Web moving speed
μ	Mass ratio; $m/\rho c$ for sheet; $m/\rho d$ for web
ρ	air density